Design and Optimization of Wafer Level Compression Molding Process for One Chip Plus Multiple Decaps

Lin Bu, Siowling Ho, Sorono Dexter Velez, Lau Boon Long,
Booyang Jung, Taichong Chai, Xiaowu Zhang

Institute of Microelectronics, A*STAR (Agency for Science, Technology, and Research)
11 Science Park Road, Singapore Science Park II, Singapore 117685
Tel: (65) 67705420 Fax: (65) 6774 5747 Email: bul@ime.a-star.edu.sg

Abstract

Decaps are the panacea to resolve the noise related issues. Due to the short distance advantage, decaps are embedded in the Fan-Out Wafer Level Package (FO-WLP) instead of PCB. These decaps, generally thicker than chips, will have a crucial influence on the molding process as well. A lot of issues are encountered in the molding process especially with lots of decaps, i.e., voids issues, incomplete filling issues and die shift issues. In an optimized design, all these issues should be prevented or reduced as much as possible. In the present paper, design flow for the wafer level molding process is demonstrated and design guidelines are provided. Three important evaluation standards are used to evaluate the design, i.e., incomplete filling, drag force and voids. Two kinds of design parameters, structure parameters (i.e., die placement, die size and thickness and etc) and process parameters (i.e., vacuum pressure, filling speed and etc) are optimized in the whole study. Optimization of these parameters helps the real wafer level molding process to be conducted smoothly.

Index terms: Decap, Molding, FO-WLP, Guidelines

I. Introduction

Embedded wafer-level packaging (eWLP) draws more and more attraction due to its inherent advantages, i.e., high density, low cost and high yields [1]. Many researchers are dedicated to wafer level

molding process, based on single chip [2, 3] as well as multiple-chip package [4-6]. Gaurav Sharma [3] used pre-compensation to reduce die shift to less than 40 μm regarding to single chip package design. The studies of multiple-chip package [4-5] suggested that a few design parameters control which could reduce the die shift issues, i.e., reducing the filling speed of the top chase, increasing the thickness of the molding compound, optimizing the initial diameter of the molding compound, selecting lower viscosity molding compound material, and using die with large surface area and low die. They enlarged the distance between the two chips and shrank the size of the chips to deal with the incomplete filling issues. Mazuir [6] et al. explored new ways to reduce die shift by enhancing the adhesion strength of silicon chips. Two types of adhesive films were successfully tested and implemented.

However, investigations on how to design the package with a chip and multiple decaps are rare. How to balance drag force in every direction in the wafer level package to avoid incomplete filling issue is the major focus in this paper. Optimizing the molding parameters to obtain a lower drag force on the whole wafer is another distinguished feature unfolded in this paper.

II. Wafer Level Molding Process

The key process in eWLP is compression molding process [4], as shown in Fig.1. The objective of this process is to hermetically seal the multiple dies/decaps into the molding compound, so that the components are protected from corrosive media, moisture and the like. The compression molding process mainly contains two steps. In the first step, the power molding compound is transformed into the liquid state by heating and then filled the mold cavity. In the second step, high packing pressure is applied on the plunger to compensate the shrinkage of the polymer molding compound during solidification. Incomplete filling and die shift due to mold flow effect are two major issues in the compression molding process, which appear in the first step and attract most of our attention in the current study.

III. Package Design

Institute of Microelectronics at the Agency for Science, Technology, and Research (A*STAR), Singapore and its industry partners developed an embedded device technology, based on a molded 8″ reconfigured wafer. The plot of package layout is illustrated in Fig.2. The package size is 8mm×8mm and the die size is 5.5mm×5.5mm. 0201 decap was 0.6mm×0.3mm with a thickness of 0.33mm. The whole package thickness is determined by decap thickness plus overmold thickness. A and B represent decap to decap distance, while C represents die to decap distance. Parametric studies would be carried out to further evaluate these parameters in the next section. The whole wafer was fully populated with 468 chips and 2808 decaps, as shown in Fig.3. Two kinds of forces are acted on the chips/decaps, i.e. drag force and adhesive force. Once drag force exceeds adhesive force, chip/decap starts to shift away from their original position. Due to a small amount of adhesive could be attached to the limited area under the bottom of decap, the value of adhesive force is very hard to achieve a very high level. Hence, it is necessary to investigate how to reduce drag force exerted on decap, which is the key to reduce the risk of decap shift.

IV. CFD Modeling

In order to further understand the molding process, computational fluid dynamics (CFD) simulation is a valuable tool. However, establishing a CFD model is a challenging task. In this paper, a 3D finite volume model is established, as shown in Fig. 3. Molding compound flows past the high power package during the molding process. The melting front is tracked by volume of fluid (VOF) method, which is proposed by Hirt and Nichols [7]. There are four reconstructed method in FLUENT software, which are modified-HRIC, QUICK, CI CSAM, compressive and geo-reconstruct. Geo-reconstruct methodology is regarded as the most accurate method in simulating the two phase flows. Therefore, geo-reconstruct methodology is adopted in the present study. The compression motion of the top mold chase is controlled by using Dynamic Mesh technique of FLUENT. In the previous studies [4-5], we use incompressible to describe

both phases. In the current study, we improve the method to be more realistic. In the whole study, only one phase, molding compound, is incompressible. The other phase, void, is regarded as the incompressible material and complies idea gas law. The governing equations and material properties of molding compound are included in section V and section VI. In the previous studies [4-5], we focus on detecting the most critical zone. However, our emphasis has been switched to use drag force of the most critical zone to optimize our design.

Fig.4 shows the air vents distribution from the real wafer. 24 air vents are evenly distributed at the edge of the wafer. The size of each vent is 3mm×2.5mm×0.03mm. Operating pressure and gas density in the simulation are both zero. Two kinds of boundary conditions are applied on the 24 vents, i.e., 101325 Pa and 0 Pa.

The modeling consists of the following assumptions:

1. A three-dimensional, time-dependent analysis will be performed on a numerical model of the reconfigure wafer with fully populated with 468 packages;
2. The molding temperature is assumed as constant during the compression stage and adiabatic condition is applied throughout the model.
3. Molding compound is assumed to be fully melted at the initial time.

Simulation flow for wafer level molding process is shown in Fig.5. Material selection and characterization is done in the first step, and then initial geometrical parameters and initial process parameters are setup in the subsequent steps (step2 and step3). Combining all the simulation parameters in the first three steps and using VOF method and dynamic mesh technology in FLUENT, the numerical simulation is carried out in step 4. Finally the initial results are obtained in step5. If the results have any confliction with complete filling, voids free or low drag force, the simulation parameters in the first three steps must be optimized in step6.

V. Governing Equations

The equation for the conservation of mass, or continuity equation, shared by the two phases, can be written as follows [8],

$$\frac{\partial \rho}{\partial t} + \nabla \cdot (\rho \vec{v}) = 0 \quad [1]$$

Conservation of momentum in an inertial (non-accelerating) reference frame, also shared by the two phases, is described by,

$$\frac{\partial}{\partial t}(\rho \vec{v}) + \nabla \cdot (\rho \vec{v} \vec{v}) = -\nabla p + \nabla \cdot (\bar{\bar{\tau}}) + \rho \vec{g} \quad [2]$$

Where p is the static pressure, $\bar{\bar{\tau}}$ is the stress tensor, and $\rho\vec{g}$ is the gravitational body.

The VOF model treats energy, h, and temperature, T, as mass-averaged variables. The properties ρ and k_{eff} (effective thermal conductivity) are shared by the phases. The source term, S_h, contains the contribution from radiation, as well as any other volumetric hear sources.

The compressible fluid complies the idea gas law,

$$\rho = \frac{p}{RT} \quad [3]$$

The transport equation is determined by,

$$\frac{\partial(\alpha\rho)}{\partial t} + \nabla \cdot (\alpha \rho \vec{v}) = 0 \quad [4]$$

$$\begin{cases} \alpha = 0, & represents\ the\ compressible\ gas; \\ \alpha = 1, & represents\ the\ incompressible\ molding\ compound; \\ 0 < \alpha < 1, & represents\ the\ interface. \end{cases}$$

The properties appearing in the transport are determined by the presence of the component phases in each control volume. In a two-phase system, if the phases are represented by the subscripts l and g, the density in each cell is given by,

$$\rho = \alpha_l \rho_l + (1 - \alpha_l)\rho_g \quad [5]$$

VI. Molding Compound Material Properties

Viscosity is one of the key material properties, precisely capturing the joint impact of shear rate and temperature. The measured viscosity is fitted using the following extended Macosko's model [9],

$$\eta(\dot{\gamma}, T) = \frac{\eta_0(T)}{1+\frac{\eta_0(T)\dot{\gamma}}{\tau^*}}\left(\frac{\alpha_g}{\alpha_g-\alpha}\right)^{c_1+c_1\alpha}$$

$$\eta_0(T) = Bexp\left(\frac{T_b}{T}\right) \quad [6]$$

Where α is the degree of cure, T the temperature, and n, τ^*, B, T_b, C_1, C_2, and α_g are the fitting constants.

As curing effect is mostly occurred in the packing stage, the behavior of molding compound is reduced to Cross Model in equation [8], which can capture the shear rate sensitivity of most material families.

$$\eta(\dot{\gamma}, T) = \frac{\eta_0(T)}{1+\frac{\eta_0(T)\dot{\gamma}}{\tau^*}} \quad [7]$$

VII. Results and Discussion

This section mainly includes four sections. In section *A* and section *B*, two key design standards, i.e., incomplete filling and drag force, are used to evaluate the die and decap placement. In section *C*, after the layout is secured, drag force is further used to determine the thickness of the die. In section *D*, the process parameters are eventually optimized in the whole process.

A. Evaluating decap layout in the measurement of incomplete filling

In order to obtain a good package design, decaps deposited along two adjacent sides and two opposite sides of the chip are compared in the present paper, as shown in Fig.6. In order to evaluate the feasibility of the two designs properly, similar conditions are used in two designs, i.e. chip thickness is 0.2 mm, filling speed is 197μm/s and over mold thickness is 100μm, etc. Fig.7 shows the evolvement of the molding compound at the stage of 90% filling for the two cases. Fig.7 (a) displays the results of balanced design. Molding compound evolves symmetrically in each direction and no sign of incomplete filling is seen. Fig.7 (b) displays the results of unbalanced design. It can be seen the flow evolves faster in the vertical direction

than the horizontal direction. This is mainly due to decaps are placed in the horizontal direction, so large gaps are left in the vertical direction with less flow resistance. Thus, balanced design dominates unbalanced design on this level.

For both cases, the lowest velocity appears at the center of the wafer, while the highest velocity appears at the peripheral. The velocity in the vertical direction is slightly higher than that in the horizontal direction for unbalanced design, as shown in Fig.8 (a). However, the velocity distribution is more uniform at the 24 vents for balanced design, as shown in Fig.8 (b).

B. Evaluating decap layout in the measurement of drag force

First of all, the design should be balanced and cause no incomplete filling issues. Once this requirement is fulfilled, another parameter, drag force, is used as the second guideline to evaluate the design. Two balanced design is demonstrated in Fig.9. The two designs are both perfect in the respect of incomplete filling. In the previous study [5], the maximum drag force appears at the last or the last two dies at the peripheral. Thus, we use drag force at last three dies and decaps around them to evaluate the design. The numbering of decap-1-1 to decap-3-6 was shown in Fig.3. Fig.10. shows the maximum drag force results from decap-1-1 to decap-3-6 for both conditions. Drag force of 12-decap design is much higher than 6-decap design. Therefore, 6-decap design are finally chosen in the real process.

Finally, further improvement is carried out to see the impact of die to decap distance C, as shown in Fig.2. Two values of C are compared, i.e. C=0.2 mm and C=0.8 mm, as shown in Fig.11. The maximum drag force is higher for C=0.2 mm than C=0.8 mm. Thus, larger decap to chip distance is favorable due to the lower drag force advantage. In the real case, we adopted our 6-decap balanced package design to the 12-inch wafer molding, as shown in Fig 12(a). The resistors are placed at the designated location on the side of the dummy dies. The wafer is fully molded without any mold related defects, as shown in Fig.12 (a) and Fig.12 (b).

C. Evaluating die thickness in the measurement of drag force

Fig.13 illustrates drag force per unit area for the chip thickness changed from 0.3 mm to 0.56 mm. It can be seen that drag force on the vertical decaps is reduced significantly as the chip thickness increases. However, drag force on the horizontal decaps is slightly increased by increasing the die thickness. This is mainly due to the vertical decaps are protected by the chips. Larger thickness of the chip results in higher protection and lower drag force. However, the horizontal decaps are not protected by the chips. Fluid flows directly from the center to the peripheral of the wafer. The results demonstrate that increasing the chip thickness can reduce drag force only in the vertical direction not the whole wafer. Therefore, increasing the thickness of the chip is not an effective way to reduce drag force in the wafer level molding process.

D. Evaluating the process parameters in the measurement of both voids & drag force

After the size and the layout are secured in the design, the next step is to evaluate the process parameters. Vacuum is worth to study due to voids are easily to be generated at the edge of the wafer. If the working condition is the atmospheric pressure at the edge of the wafer, the result of Fig.14.(a) will be formed. Voids are formulated at the edge of the wafer and cause voids issues. With applying 100kPa vacuum pressure, the voids are completely disappeared, as shown in Fig.14.(b).

Fig.15 shows drag force comparison for different filling speed. A two-step filling profile of the top mold with high velocity values of 394 μm/s & 262.8 μm/s as well as a one-step filling speed with a low velocity value of 31 μm/s are studied in the present paper. The value of drag force reduces significantly in both the vertical and horizontal directions when the filling speed is reduced from 394 μm/s & 262.8 μm/s to 31 μm/s. Therefore, lower velocity of the top mold chase is favorable in the molding process.

VIII. Conclusion

Molding is the major process in FO-WLP. In the present paper, a deep insight into the package design regarding to the optimized molding process has been presented. Some important conclusions and recommendations from this paper can be summarized as follows.

1. The design process flow can be concluded in four steps. Firstly, evaluating the die placement by incomplete filling is very crucial. Secondly, the balanced design can be further improved by reducing drag force. Thirdly, after the layout is secured, drag force is used to determine the size and the thickness of the die. Finally, the process parameters are eventually optimized. The structure parameters are required to be secured first and then followed by the process parameters.
2. In order to optimize the geometrical parameters, balanced design and unbanlanced design are compared and analyzed firstly. The results show that the balanced design dominates unbanlanced design in the measurement of incomplete filling. Then 6-decap design and 12-decap design are compared in the measurement of drag force. The results show that 6-decap design can reduce drag force significantly. At last, die to decap distance C is evaluated by drag force. The results show that larger C results in lower drag force.
3. In the optimization of process parameter, appropriate vacuum pressure should be chosen carefully. In the current design, 100kPa vacuum pressure is sufficient to resolve the voids issue. The speed of the top mold chase is the key parameter in reducing the value of drag force up to 4-5 times.
4. Summarized in the previous study [5], die shift is attributed to two major reasons, fluid effect and CTE mismatch. From fluid point of the view, die shift could be reduced by proper structure parameters and process parameters. From mechanical point of the view, die shift could be reduced by selecting the proper material properties. These two kinds of work can be conducted separately.

These findings will form the basic design and optimization guidelines for the compression molding process of one chip coupled with multiple decaps embedded wafer level packaging as well as other wafer level compression molding processes.

Acknowledgments

This work has been carried out as part of the 12th Electronics Packaging Research Consortium (EPRC-12) led by the Institute of Microelectronics (IME), a research institute of the Agency for Science, Technology and Research (A*STAR). The members of the consortium include EVG, AJINOMOTO, ACADEMY OF PUBLIC SECURITY TECHNOLOGY, HEFEI and TOKYO OHKA KOGYO. The authors are grateful to members of EPRC 12-EMWLP Project as well as IME staffs who had contributed and made this work possible.

References

1. I.-S. Kang, G.-J. Jung, and B.-Y. Jeon, "Wafer level embedded system in package (WL-eSiP) for mobile applications," in Proc. 60th Electron.Compon. *Technol. Conf.*, Jun. 2010, pp. 309–315.
2. C. H. Khong, A. Kumar, X. W. Zhang, "A Novel Method to Predict Die Shift during Compression Molding in Embedded Wafer Level Package," *Electronic Components and Technology Conference*, 2009, pp. 535-541.
3. S. Gaurav, K. Aditya, S. R. Vempati, "Solutions Strategies for Die Shift Problem in Wafer Level Compression Molding," *IEEE transactions on components packaging and manufacturing technology*, vol. 1, no. 4, (2011), pp. 502-509,.
4. L. Ji, Dexter, T. C. Chai, X. W. Zhang, "3-D Numerical and Experimental Investigations on Compression Molding in Multichip Embedded Wafer Level Packaging," *IEEE Transactions on components, packaging and manufacturing technology*, vol. 3, no. 4, (2013), pp. 678-687.
5. Lin Bu, Siowling Ho, Dexter, Taichong Chai, Xiaowu Zhang, "Investigation on Die Shift Issues in the 12 Inch Wafer Level Compression Molding Process," *IEEE Transactions on components, packaging and manufacturing technology*, online.

6. J. Mazuir, V. Olmeta, M. Yin, “Evaluation and Optimization of Die-shift in Embedded Wafer-Level Packaging by Enhancing the Adhesion Strength of Silicon Chips to Carrier Wafer,” *13th Electronics Packaging Technology Conference*, 2011, pp. 747-751.
7. C. W. Hirt, B. D. Nichols, “Volume of Fluid (VOF) Method for the Dynamics of Free Boundaries,” J. Comp. Phys., Vol.39, pp. 201–225, 1981.
8. Rohsenow W. M., Hartnett J.P., Garnic E.N., “Handbook of Heat Transfer Fundamentals”. 2nd ed. New York: McGraw-Hill, 1985
9. Castro, J. M., and Macosko, C. W., “Kinetics and Rheology of Typical Polyurethane Reaction Injection Molding Systems, ” SPE Tech. Pap., Vol.26, pp. 434–438, 1980.

FIGURE CAPTION LIST

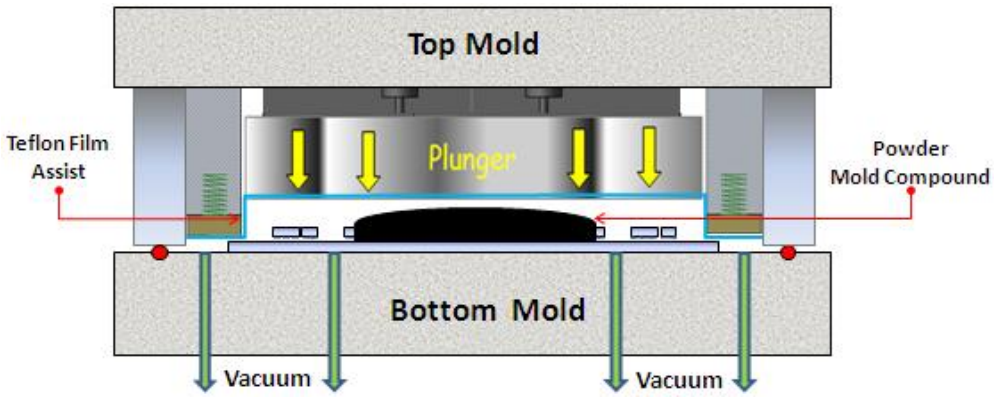

Fig.1 Schematic cross-section for compression molding structure

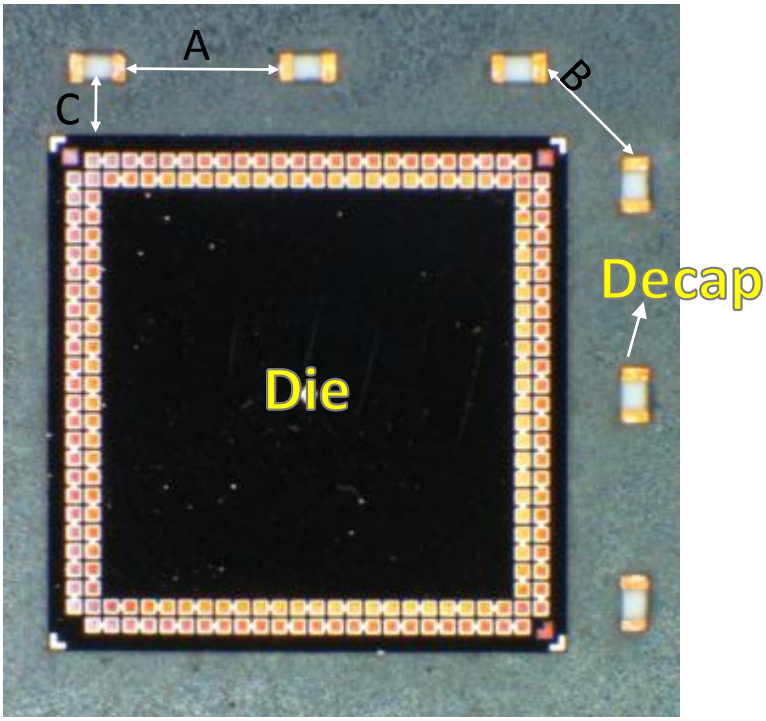

Fig.2 Package layout

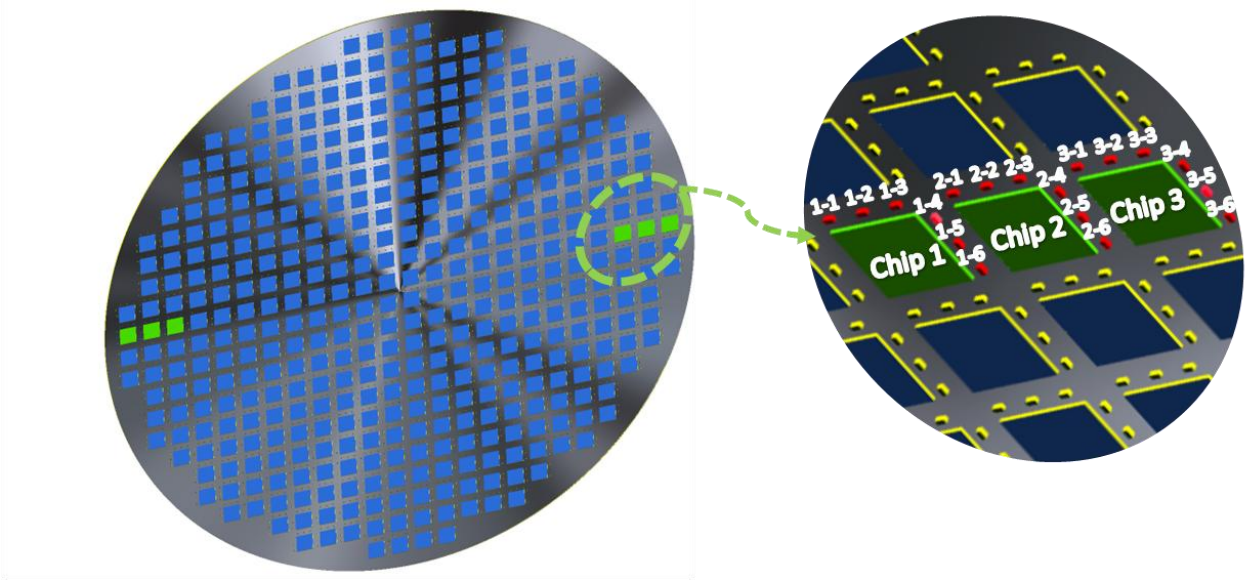

Fig. 3: CFD model of the reconfigured wafer with fully populated 468 packages

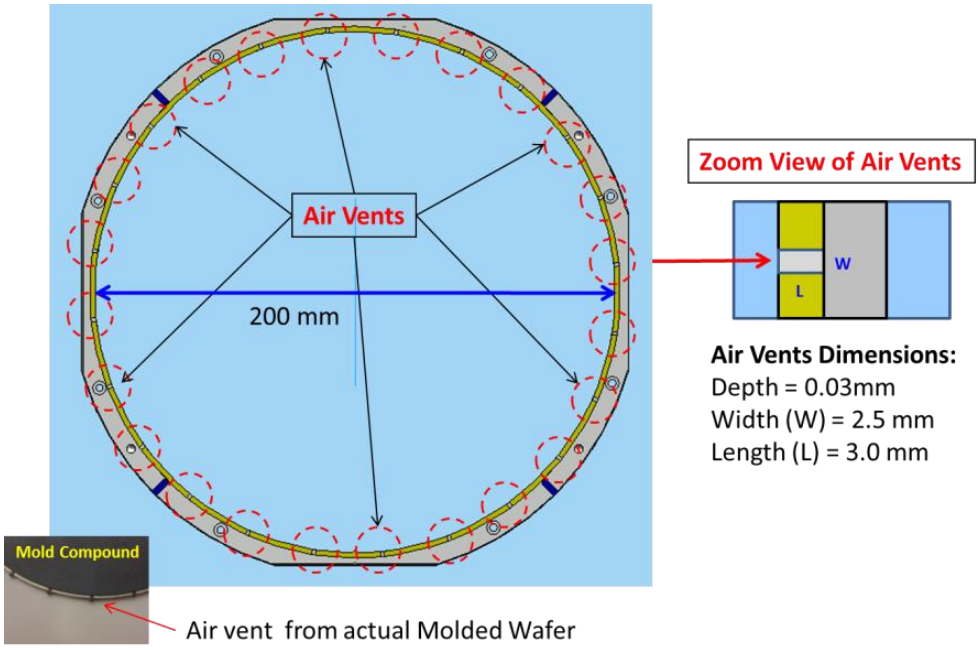

Fig.4 Air vents distribution

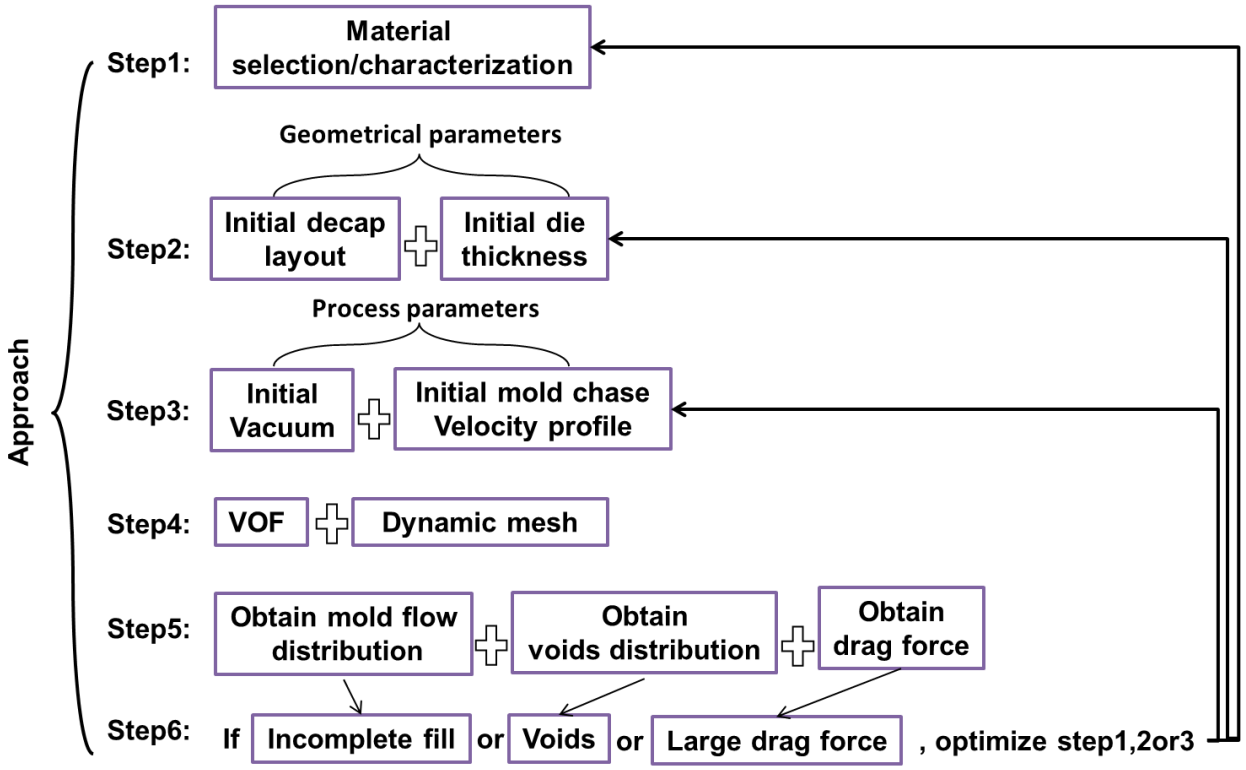

Fig.5 Simulation flow for wafer level compression molding process

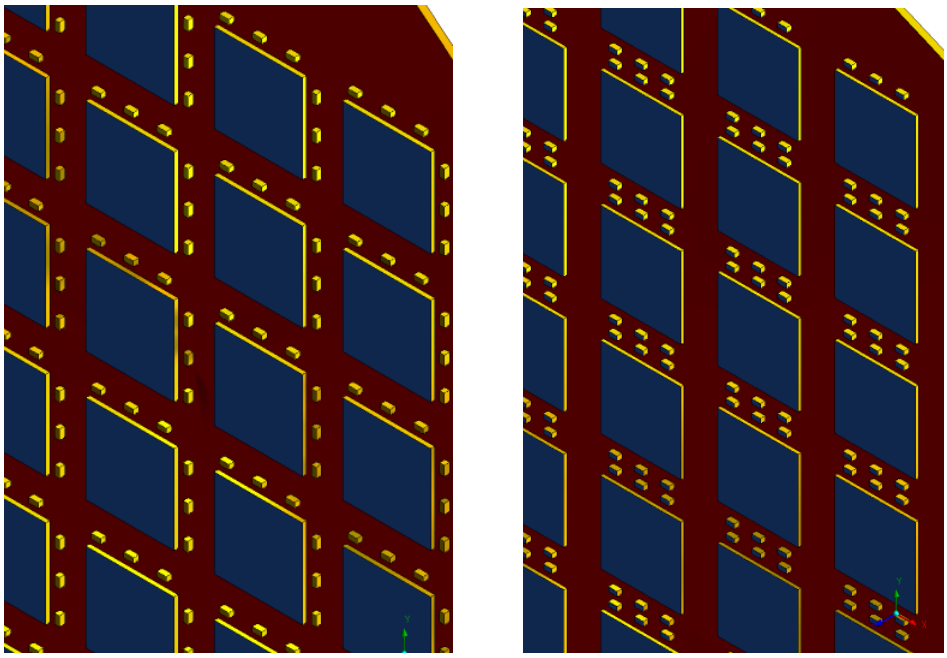

(a) Balanced package design (b) Unbalanced package design

Fig.6. Comparison balanced and unbalanced package design

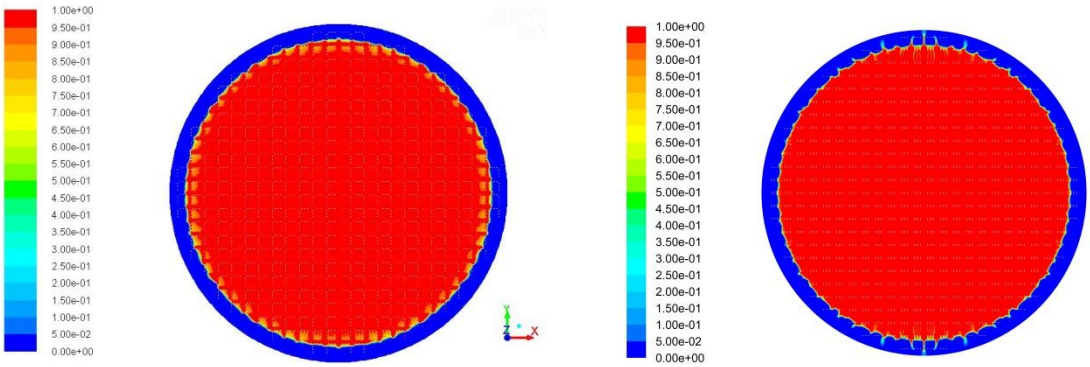

(a) Balanced package design (b) Unbalanced package design

Fig.7. Molding compound melting front comparison for balanced and unbalanced design

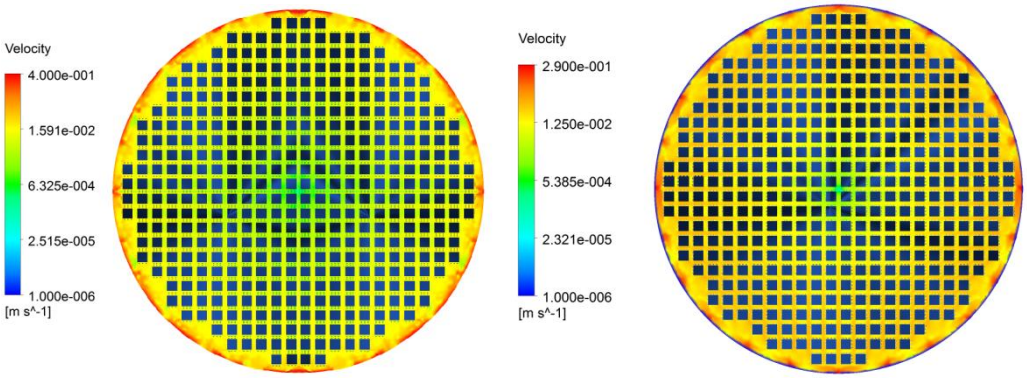

(a) Unbalanced design (b) Balanced design

Fig.8 Velocity comparison for unbalanced and balanced design

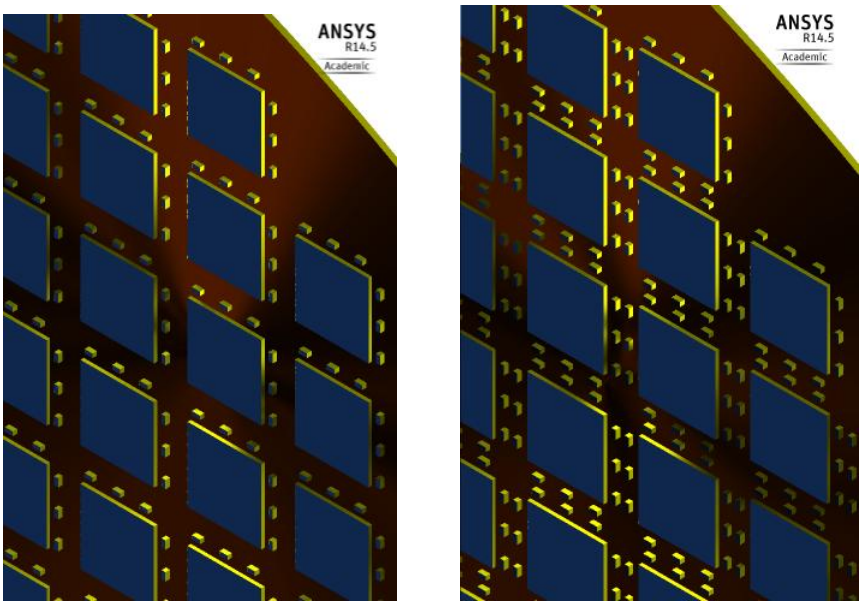

(a) 6-decap package (b) 12-decap design

Fig.9. Geometrical comparison for 6 decap and 12 decap desgin

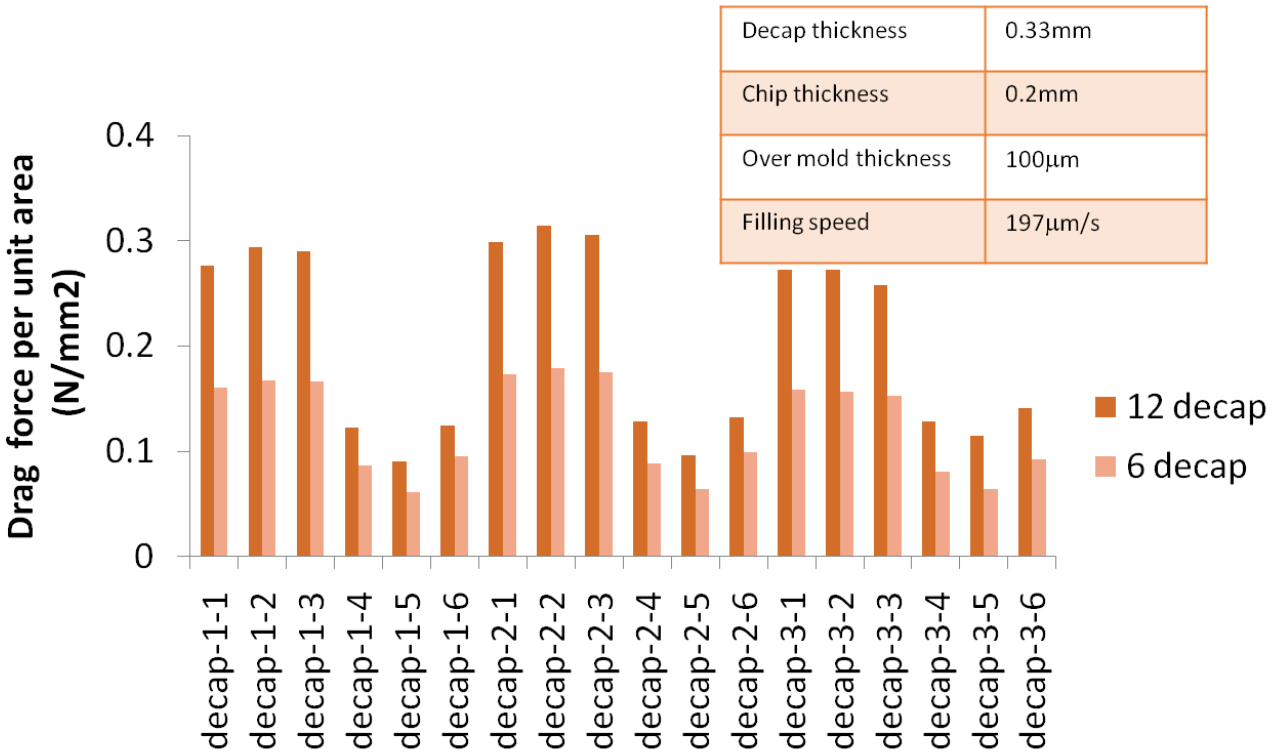

Fig.10. Drag force results comparison for 6 decap and 12 decap dsign

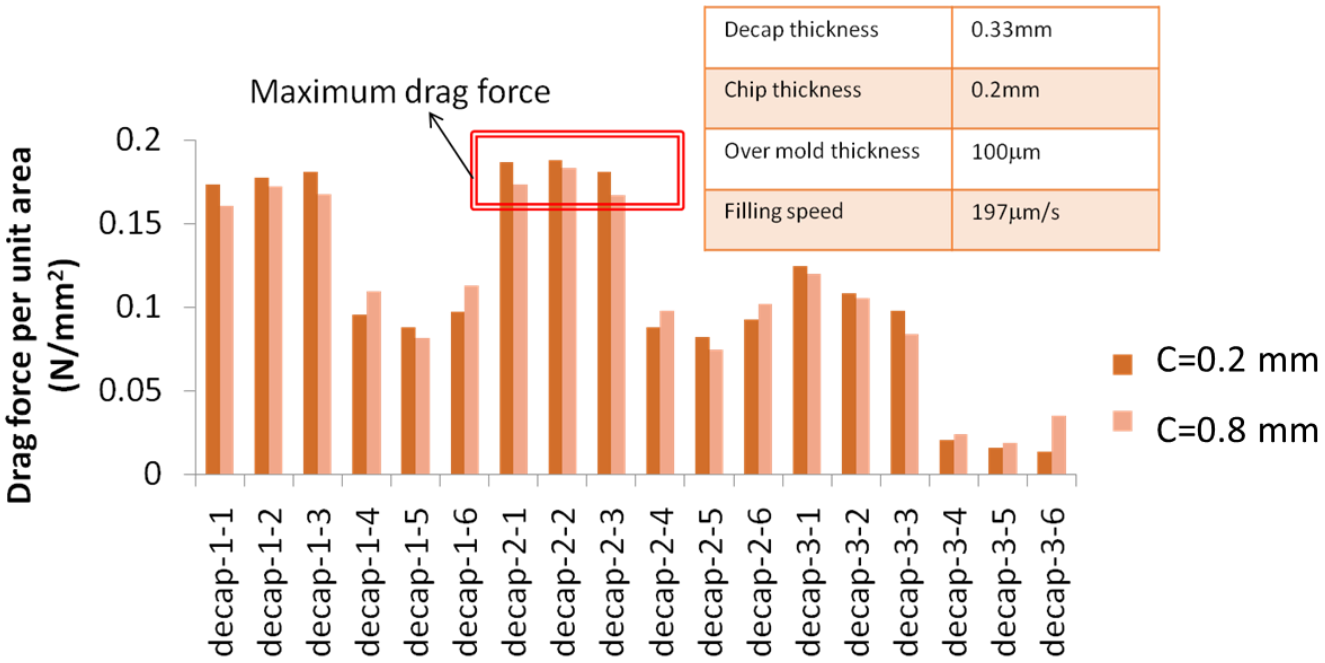

Fig.11. Comparison of drag force per for different decap to die distance

(a) Before molding

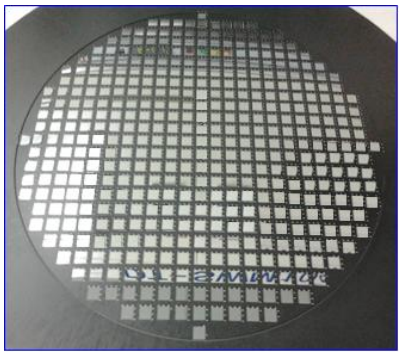

(b) After molding

Fig.12 Experimental inspection for balanced package design

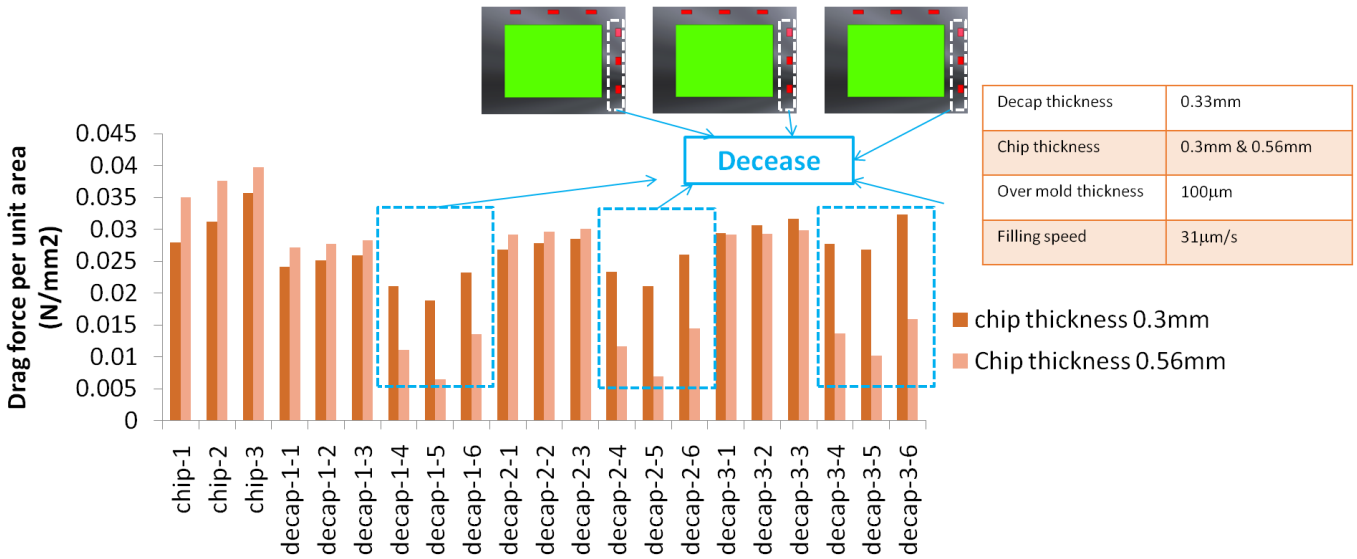

Fig.13. Comparison of drag force per unit area for different chip thickness

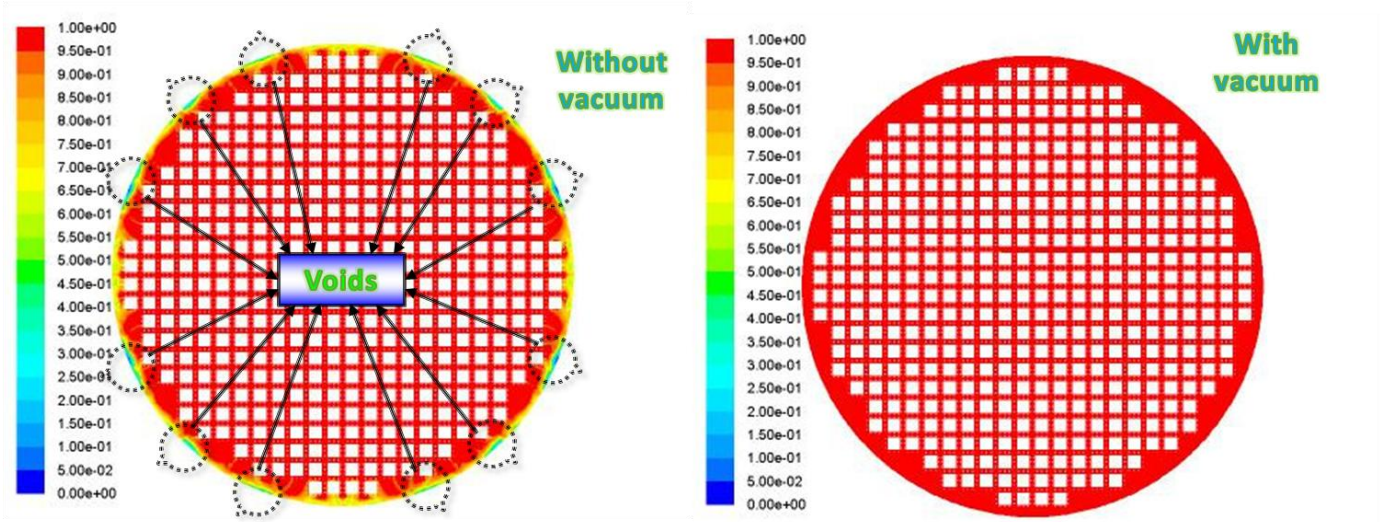

(a) Without vacuum (b) With vacuum

Fig.14. Comparison of the process condition with and without vacuum

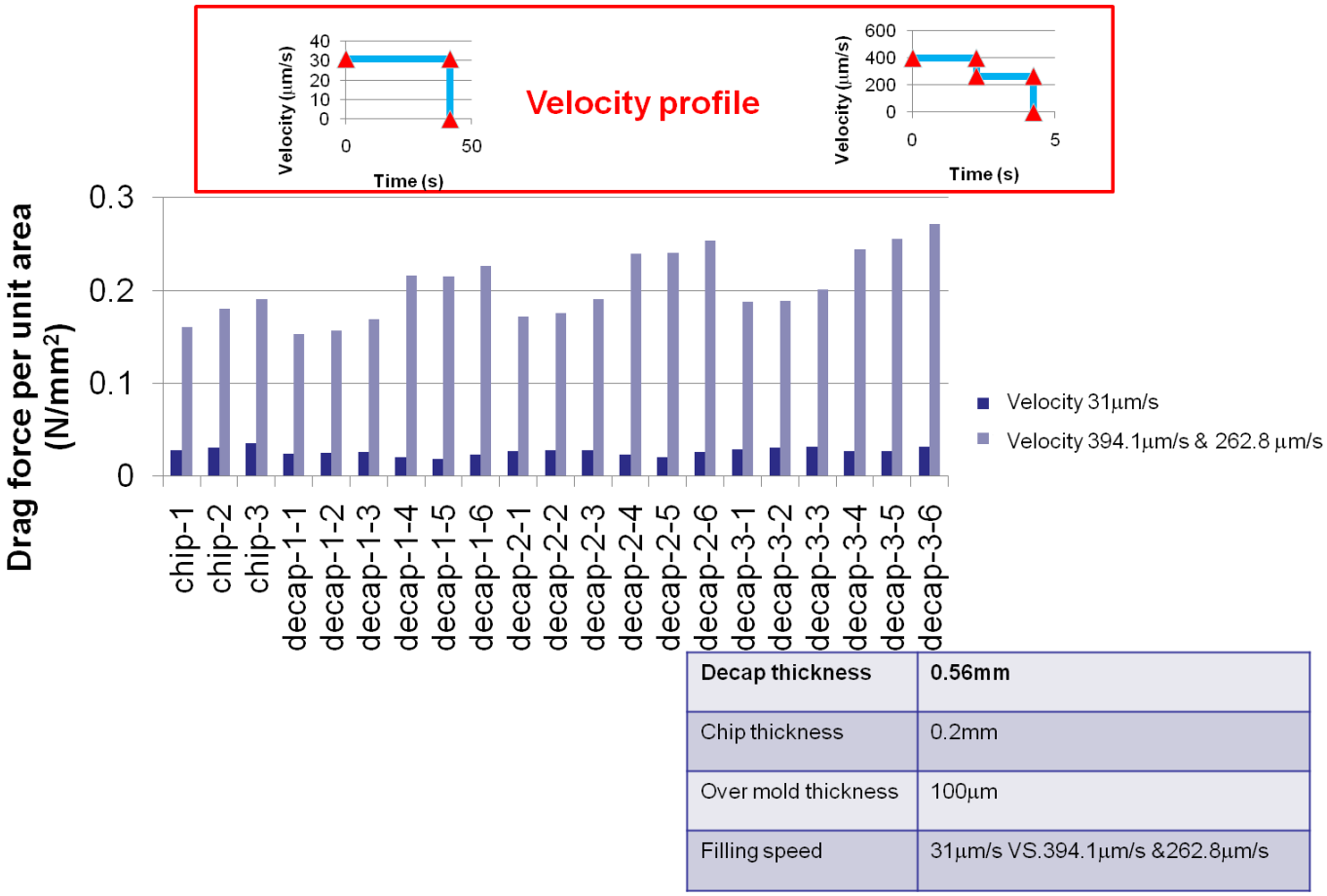

Decap thickness	0.56mm
Chip thickness	0.2mm
Over mold thickness	100μm
Filling speed	31μm/s VS.394.1μm/s &262.8μm/s

Fig.15. Comparison of drag force per unit area for different filling speed